Electronic Supplementary Information

Low Carbon Strategies for Sustainable Bio-alkane Gas Production and Renewable Energy

Mohamed Amer,‡[a] Emilia Z. Wojcik,‡[a] Chenhao Sun,‡[a] Robin Hoeven,‡[ab] John M. X. Hughes,‡[a] Matthew Faulkner,‡[a] Ian Sofian Yunus,[c] Shirley Tait,[a] Linus O. Johannissen,[a] Samantha J. O. Hardman,[a] Derren J. Heyes,[a] Guo-Qiang Chen,[ad] Michael H. Smith,[b] Patrik R. Jones,[c] Helen S. Toogood[a] & Nigel S. Scrutton[abd]*

[a]EPSRC/BBSRC Future Biomanufacturing Research Hub, BBSRC/EPSRC Synthetic Biology Research Centre, Manchester Institute of Biotechnology and School of Chemistry, The University of Manchester, Manchester, M1 7DN, UK.

[b]C3 Biotechnologies Ltd, The Railway Goods Yard, Middleton-in-Lonsdale, Lancashire, LA6 2NF, UK.

[c]Department of Life Sciences, Imperial College London, Sir Alexander Fleming Building, London SW7 2AZ, UK.

[d]School of Life Sciences, Tsinghua University, 100084 Beijing, China.

‡ Each author contributed equally to this manuscript

*Corresponding author: nigel.scrutton@manchester.ac.uk

Table of Contents

Supplementary Figures

Supplementary Tables

Supplementary Figures

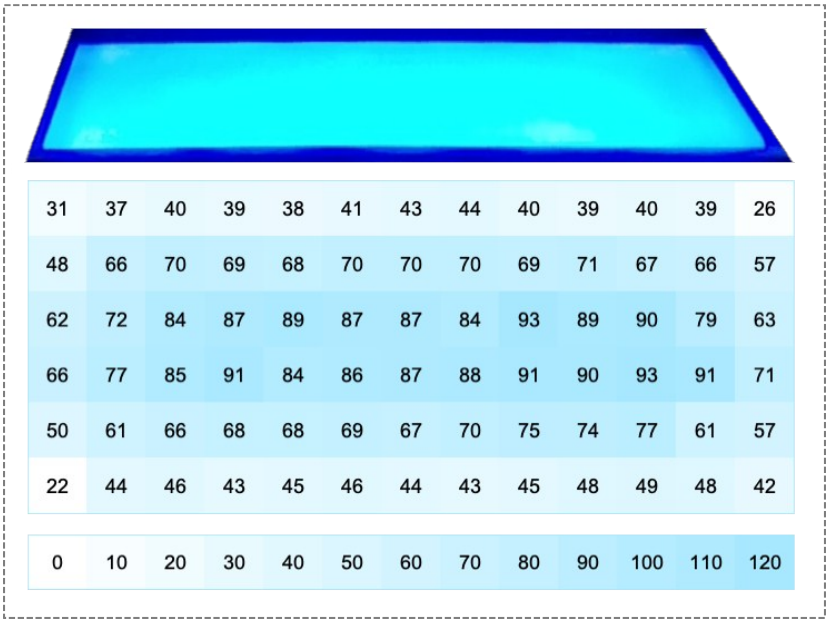

Fig. S1. Custom built blue light LED array. It is composed of 480 individual blue LEDs, giving an area of 396 cm^2 of relatively consistent light intensity and a fixed average culture-to-LED distance of 8 cm. Light intensity was measured with a Li-Cor light meter with a Quantum sensor, with background light value (room lights) subtracted. Values are in μmol photons/s/m^2 or μE. Each square is approx. 3 x 3 cm.

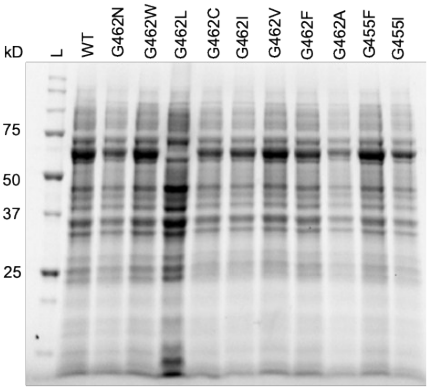

Variant	Concentration relative to WT
WT	1.00
G462N	0.64
G462W	1.08
G462L	*No visible band*
G462C	0.67
G462I	0.73
G462V	1.05
G462F	0.75
G462A	0.42
G455F	1.11
G455I	0.56

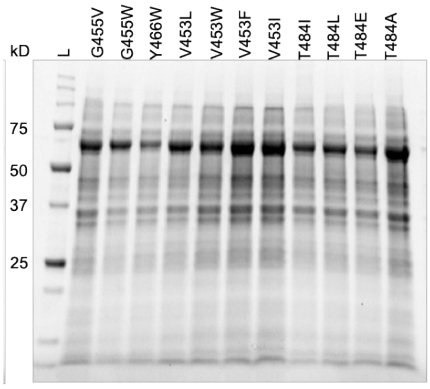

Variant	Concentration relative to WT
G455V	0.87
G455W	0.76
Y466W	0.49
V453L	1.03
V453W	0.85
V453F	1.27
V453I	1.20
T484I	0.73
T484L	0.83
T484E	0.68
T484A	1.29

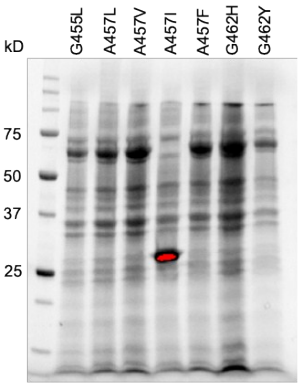

Variant	Concentration relative to WT
G455L	0.42
A457L	0.70
A457V	0.97
A457I	*No visible band*
A457F	0.86
G462H	1.02
G462Y	0.51

Fig. S2. Expression of various CvFAP variants in *E. coli*. Protein from equal quantities of soluble cell lysate was resolved by SDS PAGE, visualized with a BioRad Gel Doc™ EZ Imager, and relative quantities of bands corresponding to CvFAP determined using instrument software. L, molecular mass ladder; WT, $CvFAP_{WT}$.

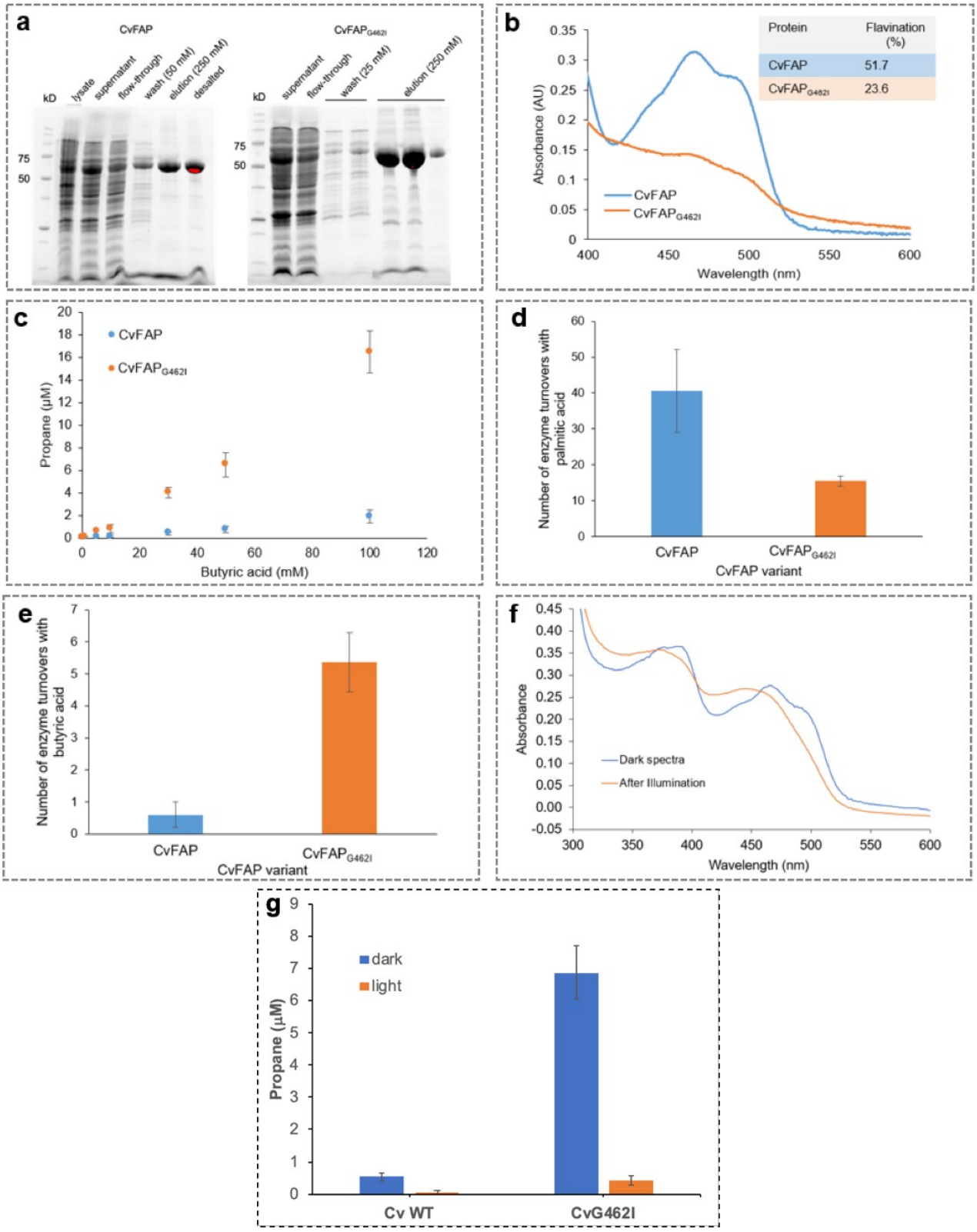

Fig. S3. Purification and activity assays of CvFAP and CvFAP$_{G462I}$. a) SDS-PAGE gels of CvFAP and CvFAP$_{G462I}$ purifications, showing soluble cell lysate, supernatant, purification flow-through, column washes, elution (imidazole concentrations in mM) and desalted protein. Absorbance spectra of b) purified CvFAP$_{WT}$ and CvFAP$_{G462I}$ normalised to 280 nm. Protein concentration was measured using absorbance at 280 nm using the extinction coefficient ε = 63 830 M^{-1} cm^{-1}, and FAD-bound protein concentration was measured using absorbance at 460 nm, using the flavoprotein extinction coefficient (ε = 11,300 M^{-1} cm^{-1}). The flavination percentage of each protein (amount of FAD-bound protein in the total protein sample) was determined by calculating the 460 nm/280 nm ratio. The absorbance spectra show that the flavination of CvFAP is higher

than that of $CvFAP_{G462I}$. c) Activity assay of 1 µM $CvFAP_{WT}$ and $CvFAP_{G462I}$ with different concentrations of butyric acid with overnight incubation under a blue LED array. Protein concentrations calculated for the enzyme assays were based on the concentration of FAD-bound protein. $CvFAP_{G462I}$ has higher activity with butyric acid than CvFAP as shown by propane production. d) and e) The number of enzyme turnovers was calculated by measuring the amount of pentadecane (d) or propane (e) produced after illuminating samples containing 1 µM enzyme and either 100 µM palmitic acid (d) or 50 mM butyric acid (e) with a blue LED array. Samples were illuminated for 45 minutes (d) or 90 minutes (e), after which no further product was formed. Data are the average of three technical replicates. f) Absorbance spectra of CvFAP before and after light exposure with the blue LED for 15 minutes, showing changes in the flavin peak upon illumination. To standardize culture light exposure, we assembled a custom-built LED array light source composed of 480 individual blue LEDs, giving an area of 396 cm^2 of relatively consistent light intensity and a fixed average culture-to-LED distance (8 cm; **Fig. S1**). The average PFD (78 ± 10 µmol photons/s/m^2) was similar to the average for the 470 nm LED, but importantly it showed a higher consistency of light over a wider area, and its maximal wavelength was close to the absorbance maximum of $CvFAP_{WT}$. This new light source gave greater reproducibility between replicate samples, allowing comparative studies to be performed. g) Photoinactivation of CvFAP. Purified $CvFAP_{WT}$ and G462I variant were either kept in the dark or exposed to high intensity blue light for 15 min (455 nm). Aliquots (1 ml) were sealed in glass vials (4 mL) with 50 mM butyric acid, and illuminated under the LED array at 30 °C (180 rpm) for 90 min.

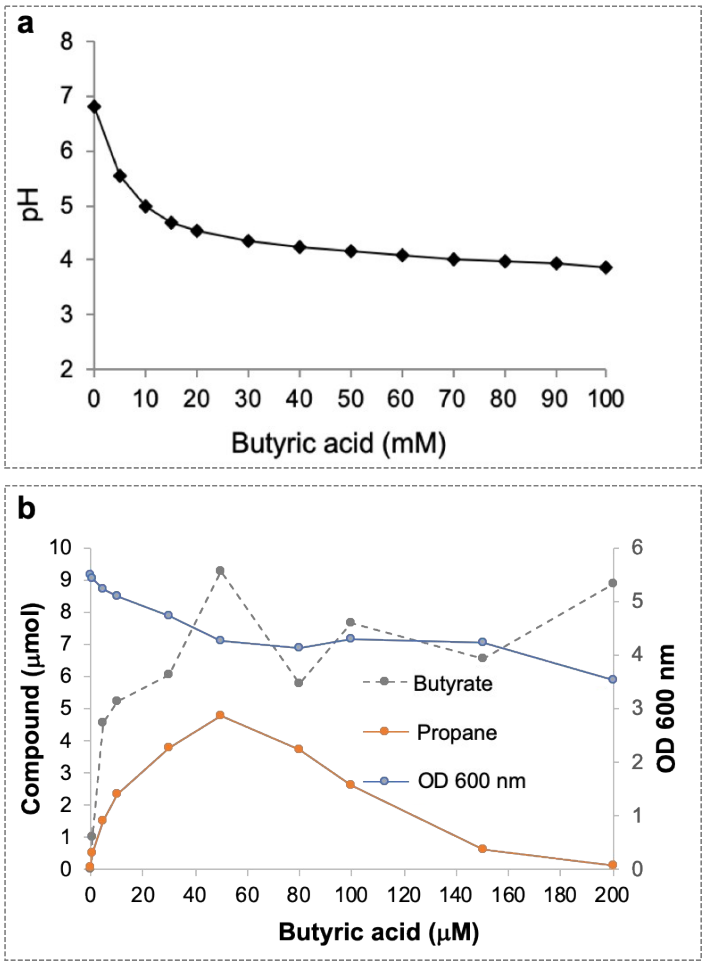

Fig. S4. Effect of butyrate concentration on propane production. a) Effect of unbuffered butyric acid addition to culture medium (LB). Cultures of *E. coli* BL21(DE3) containing pETM11-CvFAP variants and b) G462V in LB broth with kanamycin (50 µg/mL) were inoculated at 1% volume from overnight starter cultures and grown for a further 6 h at 37 ºC at 180 rpm. CvFAP expression was induced with IPTG (0.1 mM), butyric

acid was then added. Triplicate aliquots (1 mL each; technical replicates) were sealed in 5 mL glass vials and incubated at 30 ºC for 16-18 h at 200 rpm, illuminated continuously under a blue LED panel. Headspace gas was analyzed for propane content using a Micro GC (100 ms injection) with an Al_2O_3/KCl column. Error bars represent one standard deviation of the data (n=3). Data points: black = butyrate consumption; red = propane production; blue = culture OD600 nm.

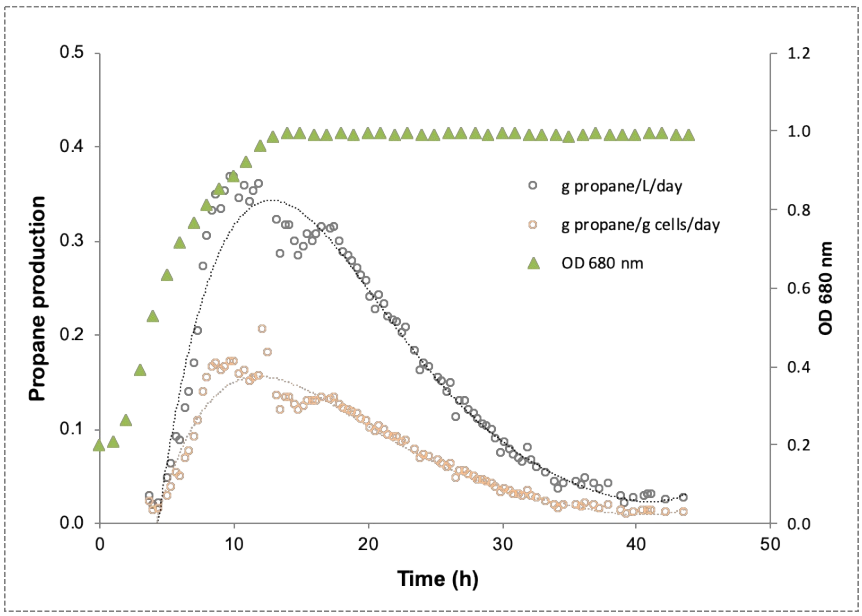

Fig. S5. Propane production by *Halomonas* in a photobioreactor. Cultures were grown in high-salt glycerol medium at pH 6.8 (5 g/L yeast extract, 1 g/L glycerol, 60 g/L NaCl, 50 µg/mL spectinomycin and 0.5 mL/L antifoam; 400 mL) at 30 °C with maximal stirring and 1.21 L/min aeration. For crude medium, seawater with supplemental NaCl and biodiesel waste glycerol were used in place of laboratory grade reagents. $CvFAP_{G462V}$ expression was induced with IPTG (0.1 mM) at mid-log phase, followed by the addition of sodium butyrate (60 mM pH ~6.8) and blue light exposure (1656 µmol/s/m^2 photons) for up to 48 h. Culture growth was maintained at OD 680 of 1.0 by automated feed addition. Propane production was monitored every 20 minutes by automated headspace sampling using a Micro GC.

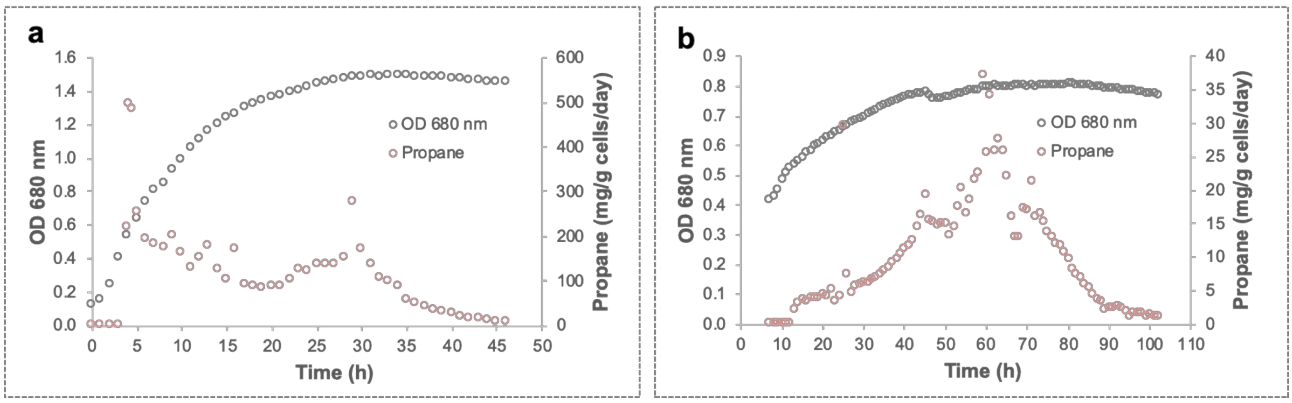

Fig. S6. *Halomonas* plasmid-borne or genomically integrated propane production. Propane production via **a)** plasmid-borne constitutively expressed $CvFAP_{G462V}$ or **b)** chromosomally integrated IPTG-inducible $CvFAP_{G462V}$ in a flat-bed photobioreactor. Cultures were grown in high-salt glycerol medium at pH 6.8 (5 g/L yeast extract, 10 g/L glycerol, 60 g/L NaCl, 50 μg/mL spectinomycin and 0.5 mL/L antifoam; 400 mL) at 30 °C with maximal stirring and 1.21 L/min aeration. CvFAP expression was induced with IPTG where required (0.1 mM) at mid-log phase, followed by the addition of sodium butyrate (60 mM pH ~6.8) and blue light exposure (1656 μmol/s/m^2 photons) for 48-102 h. Propane production was monitored every 20 minutes by automated headspace sampling using a Micro GC. The decline in propane production after ~ 60-80 h is due to loss of cell viability due to prolonged light exposure.

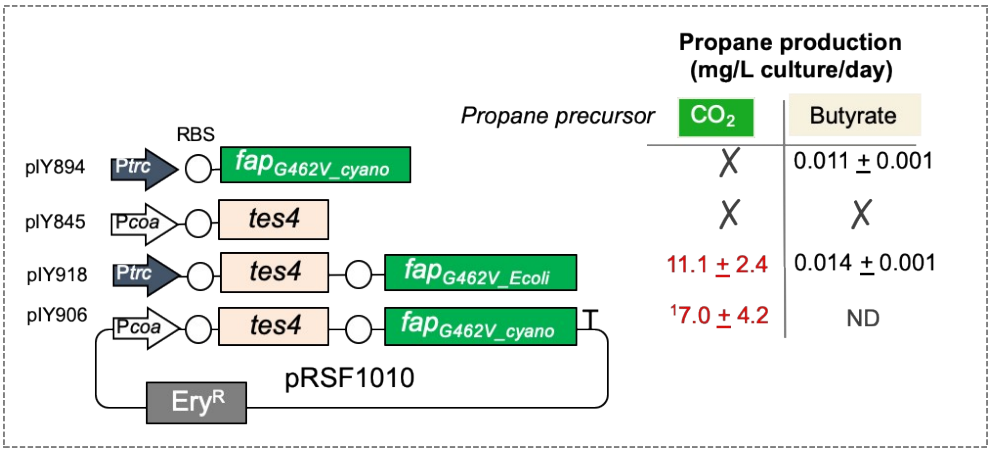

Fig. S7. Photoautotrophic propane production. Propane production from plasmid constructs in *Synechocystis* Δ*aas* from CO_2 or butyrate feeding. Culture growth was performed in batch mode (sealed vials) in the presence or absence of 10 mM butyrate, and under standard photosynthetic conditions in a photobioreactor (see Experimental section). The following constructs were generated: *i*) pIY894: Ptrc::fap_{G462V_cyano}; *ii*) pIY918: Ptrc::*tes4*, fap_{G462V_Ecoli}; *iii*) pIY906: Pcoa::*tes4*, fap_{G462V_cyano}; and *iv*) pIY845: Pcoa::*tes4*. Ptrc = *E. coli* promoter lacking the *lacI*, making it a constitutive promoter. Red numbers indicate propane production monitored in a photobioreactor in the absence of butyrate supply, while black numbers were obtained from batch (flask) cultures in the presence of 10 mM butyrate. [1]Propane production detected in non-induced cultures. Each data point is an average of biological triplicates. Errors represent one standard deviation of the data. Tes4 = acyl-ACP thioesterase; Ery^R = erythromycin resistance gene. ND = not determined because the higher expression of the cyanobacterial codon optimised gene $CvFAP_{G402V\_cyano}$ appeared to be toxic, and significantly reduced cell growth rates.

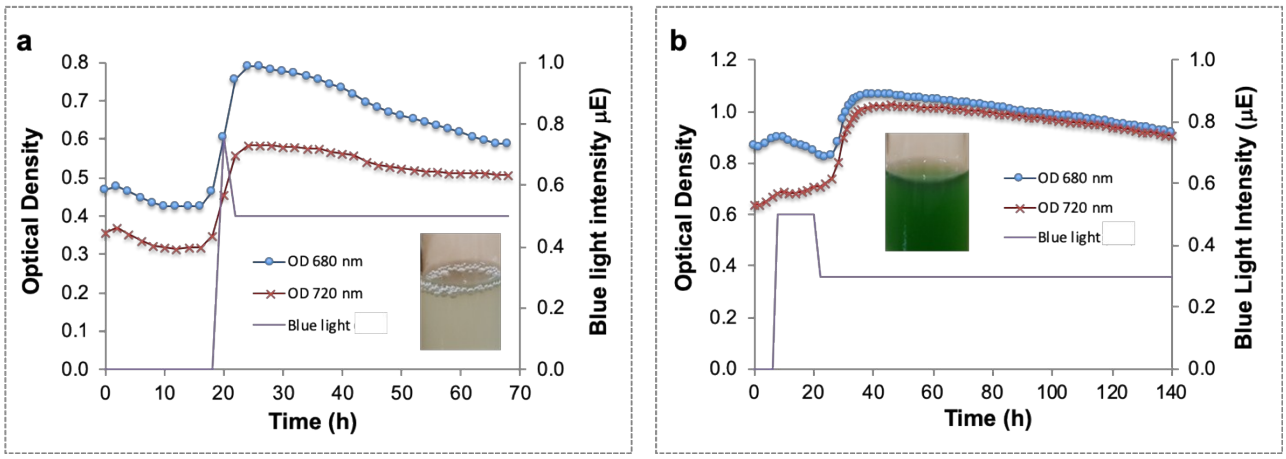

Fig. S8. Effect of blue light intensity on *Synechocystis* photobleaching. The photobioreactor (400 mL) was set up in batch mode with starter culture diluted 3:1 in fresh BG11^{+} medium (BG11 pH 8.0[1, 2] containing TES buffer and 1 g/L sodium thiosulphate) in the presence of 150 mM $NaHCO_3$. Both pH control and CO_2 supply were maintained using 1M $NaHCO_3$ in 2 x BG11^{+}. The culture was maintained at 30 °C with maximal stirring with an airflow rate of 1.21 L/min, illumination of warm white light (30 µE), automated pH maintenance (1M acetic acid in 2 x BG11^{+}) and optical density monitoring (680 nm and 720 nm). After reaching an optical density of ~0.5 (720 nm), cobalt (II) nitrate hexahydrate (150 µM) was added as required, the warm white illumination was increased to 60 µE the integral actinic blue LED light panel was activated to provide a) 800 µE blue light initially then a reduction to 500 µE or b) 500 µE blue light initially then a reduction to 300 µE. The culture was maintained at 30 °C for up to 140 hours. Inset: Culture samples at the end of the cultivation, showing photobleaching in a) but not b).

Supplementary Tables

Table S1. Putative mature[a] amino acid sequences of the synthesised proteins.

Protein	Amino acid sequence
CvFAP	MASAVEDIRKVLSDSSSPVAGQKYDYILVGGGTAACVLANRLSADGSKRVLVLEAGPDNTSRDVKIPAAIT RLFRSPLDWNLFSELQEQLAERQIYMARGRLLGGSSATNATLYHRGAAGDYDAWGVEGWSSEDVLSWFVQA ETNADFGPGAYHGSGGPMRVENPRYTNKQLHTAFFKAAEEVGLTPNSDFNDWSHDHAGYGTFQVMQDKGTR ADMYRQYLKPVLGRRNLQVLTGAAVTKVNIDQAAGKAQALGVEFSTDGPTGERLSAELAPGGEVIMCAGAV HTPFLLKHSGVGPSAELKEFGIPVVSNLAGVGQNLQDQPACLTAAPVKEKYDGIAISDHIYNEKGQIRKRA IASYLLGGRGGLTSTGCDRGAFVRTAGQALPDLQVRFVPGMALDPD**G**VSTYVRFAKFQSQGLKWPSGITMQ LIACRPQSTGSVGLKSADPFAPPKLSPGYLTDKDGADLATLRKGIHWARDVARSSALSEYLDGELFPGSGV VSDDQIDEYIRRSIHSSNAITGTCKMGNAGDSSSVVDNQLRVHGVEGLRVVDASVVPKIPGGQTGAPVVMI AERAAALLTGKATIGASAAAPATVAA
CcFAP	MAGTVASTFRRTVPSSEAATTYDYIIVGGGAAGCVLANRLTEDPSTRVLLLEAGKPDDSFYLHVPLGFPYL LGSPNDWAFVTEPEPNLANRRLYFPRGKVLGGSHAISVMLYHRGHPADYTAWAESAPGWAPQDVLPYFLKS ESQQSAVPNQDAHGYEGPLAVSDLARLNPMSKAFIKAAHNAAGLNHNPDFNDWATGQDGVGPFQVTQRDGS RESPATSYLRAAKGRRNLTVMTGAVVERILFENPAGSSTPVATAVSFIDSKGTRVRMSASREILLCGGVYA TPQLLMLSGVGPAEHLRSHGIEIVADVPAVGQNLQDHAAAMVSFESQNPEKDKANSSVYYTERTGKNIGTL LNYVFRGKGPLTSPMCEAGGFAKTDPSMDACDLQLRFIPFVSEPDPYHSLADFATAGSYLQNRANRPTGFT IQSVAARPKSRGHVQLRSTDVRDSMSIHGNWISNDADLKTLVHGVKLCRTIGNDDSMKEFRGRELYPGGEK VSDADIEAYIRDTCHTANAMVGTCRMGIGEQAAVDPALQVKGVARLRVVDSSVMPTLPGGQSGAPTMMIAE KGADLIRAAARQADAATVGAAA
ChFAP[b]	MAMRRLVYICAVATVTAAISSRSVPTSARRLIALRGGVAAAEQLAEEPWDYIIVGGGAAGCVMAERLSAAE ARVLVLEAGTDASRDLRIRVPAGLIKVFKSERDWDFTTEAGQGTSGRGIYLCRGKALGGSSCTNVMLYNRG SPADYNSWVAAGAEGWGPDSVLHYYRKSENYVGGASQYHGVDGPLSVSDVPYENELSTAFLRAAGELGYRR VHDFNDWSAPQEGFGRYKVTQRNGERCSAANAYLEGTEGRSNLCVRTGVHATRVTLEGSGDDLCAAGVEYI GADGKPSRAQLAQGGEVLLSAGAVQSPQLLMLSGIGPRAHLEEVGIEVRKELDNVGVGLADHPAVVVSCGS KKKVSVTDEIRLWGGSKTNPMALLRWLLWRRGPLTSVACEFGGFFKTKPDLKQADVQVRFVAARAMSPDGI TTLQQLGAGAKFLSGYTTQIIACRPQSTGLVRLRSSDPLAQPMLQDVHLSDDADVATLREGIKLGRQLLAA KSFDQYRDEEVYPGVAVQSDEDIDAYVRKTTHSANALVGSCRMGRVDDQAAVLDPEMRVRGVGSLRVVDAS AMPHIIGGQTCGPTIMMAEKAADLVLRQRAEINAYMQQAQAYLAASAGAATPALSPAQAA
CmFAP	MAQYDFIIVGAGAAGCVLANRLSTAQFSNGDRRYPRVLLLEAGDALAEAPYFEHIPLGFPQLIGSRLDYGF FSRENPTHLGGRGAVYLPRGRGEGGSHAISVMLVHRGSRHDYETWVKDYEALGWGPDDVLPYFKRLESNER TAQRGADGEAATALHGSDGPLRVSDQRSPNPLSLAFIEACLERGIRRNKDFNDWDHGQEGAGLFQVTQRDG RRESPATAYLQPVRSRRNLHIETNALAEHLVWSKDGRRVEGIRFIDRHGRRRAALAHCEVILAAGAINTPQ LLMLSGLGPGAHLQDFGIPVVRDLPGVGQNLQDHAAVMLSYYAPDPYGKDRDKKRIFYTERLGKDPLVLAE YFLLGRGPLTSPVCEAGAFVHTQAVIGEPSCDLQLRFVPFFSDADPYKSLGEYRSGGHVLTNTSIRPAGFG LQAVAIRPRSRGRIELATIDPRARPIIHTGWLEDKRDLQTLLSGLKLGREILSGDSMRPYRGREAFPETLE DDLVTYIRRTCHTANAIVGTARMGTGRDAVVDPELRVHGVERLRVIDASVMPKIIGGQTGVPTMMIAERGA DLVKKTWKLV
CrFAP	MASVRAAAGPAGSEKFDYVLVGGGTASCVLANKLSADGNKKVLVLEAGPTGDAMEVAVPAGITRLFAHPVM DWGMSSLTQKQLVAREIYLARGRMLGGSSGSNATLYHRGSAADYDAWGLEGWSSKDVLDWFVKAECYADGP KPYHGTGGSMNTEQPRYENVLHDEFFKAAAATGLPANPDFNDWSHPQDGFGEFQVSQKKGQRADTYRTYLK PAMARGNLKVVIGARATKVNIEKGSSGARTTGVEYAMQQFGDRFTAELAPGGEVLMCSGAVHTPHLLMLSG VGPAATLKEHGIDVVSDLSGVGQNLQDHPAAVLAARAKPEFEKLSVTSEVYDDKCNIKLGAVAQYLFQRRG PLATTGCDHGAFVRTSSSLSQPDLQMRFVPGCALDPDGVKSYIVFGELKKQGRAWPGGITLQLLAIRAKSK GSIGLKAADPFINPAININYFSDPADLATLVNAVKMARKIAAQEPLKKYLQEETFPGERASSDKDLEEYIR RTVHSGNALVGTAAMGASPAAGAVVSSADLKVFGVEGLRVVDASVLPRIPGGQTGAATVMVAERAAALLRG QATIAPSRQPVAV
CsFAP	MAPAADKYDFILVGGGTAGCVLANRLTADGSKKVLLLEAGGANKAREVRTPAGLPRLFKSALDWNLYSSLQ QAASDRSIYLARGKLLGGSSATNATLYHRGTAADYDAWGVPGWTSQDALRWFIQAENNCRGIEDGVHGTGG LMRVENPRYNNPLHEVFFQAAKQAGLPENDNFNNWGRSQAGYGEFQVTHSKGERADCFRMYLEPVMGRSNL TVLTGAKTLKIETEKSGGATVSRGVTFQVNGQDGSKHSAELAAGGEVVLCAGSIHSPQILQLSGIGPQAEL RSKDIPVVADLPGVGQNMQDHPACLSAFYLKESAGPISVTDELLHTNGRIRARAILKYLLFKKGPLATTGC

	DHGAFVKTAGQSEPDLQIRFVPGLALDPDGIGSYTAFGKMKDQKWPSGITFQLLGVRPKSRGSVGLRSDDP
	WDAPKLDIGFLTDKEGADLATLRSGIKLSREIAAEPAFGAYVGNELHPGAAASSDSAIDSFIRDTVHSGNA
	NVGTCSMGVNGNAVVDPSLRVFGIRGLRVADASVIPVIPGGQTGAATVMVAERAAEILLGSNQKQPAAAVP
	AAQPALA
GpFAP	MAPVDPAEKYDYILVGGGTAGCVLANKLSADGNKKVLVLEAGPSGDSLEVAVPAGIARLFAHPVMDWGMSS
	LTQKQLVAREIYLARGRLLGGSSGTNATLYHRGTSSDYDSWGLEGWTSKDVLDWFVKAECYGDGPKPYHGN
	SGSMNVEQPRYQNPLHEEFFRAAAAAGIPANPDFNDWSRPQDGYGEFQVAQNKGQRADTYRTYLKPALSRG
	NLKVVTGARTTKVHIEKGSSGPRARGVEFATQQFGDRYSAQLAPGGEVLMCTGAVHTPHLLMLSGVGPAAA
	LREHGVDVVADLAGVGANLQDHPAAVVAVRAKPEFEKLSVTSEIYDEKCNIKLGAVAQYLFNRRGPLATTG
	CDHGAFVRTSGSHSQPDLQMRFVPGCALDPDGVKSYIVFGELKKQGRAWPGGITLQLLAIRAKSKGSIGLK
	AADPFINPAININYFSDPADLATLKQGVRMARDIARQEPLRKYLQEETFPGERASSDSDIEEYVRRTVHSG
	NALVGTCAMGTSPAKGAVVSSSDLKVFGVEGLRVVDASVLPQIPGGQTGAATVMVAERAAALLKGQTTMAP
	SRQPVAA
PtFAP[b]	MAYDYIICGGGLAGCVLAERLSQDESKRVLVLEAGGSDYKSLFIRIPAGVLRLFRSKYDWQHETGGEKGCN
	GRNVFLQRGKILGGSSCTNVCLHHRGSAEDYNSWNIPGWTATDVLPFFKQSQKDETGRDATFHGADGEWVM
	DEVRYQNPLSKLFLEVGEAAGLGTNDDFNNWSHPQDGVGRFQVSEVNGERCSGATAFLSKAAKRSNVIVRT
	GTMVRRIDFDETKTAKGITYDLMGDDTCTVPCLKEGGEVLVTGGAIASPQLLMCSGIGPGKHLRSLGIPVV
	HDNSAVGENLQDHPAAVVSFKTPQKGVSVTSKLRLFGKTNPIPVFQWLFFKSGLLTSTGCDHGAFVRTSDS
	LEQPDLQIRFLAARALGPDGMTTYTKFRTMKTVEDGYSFQSVACRAKSKGRIRLSSSNSHVKPMIDGGYLS
	NQDDLATLRAGIKLGRMLGNRPEWGEYLGQEVYPGPDVQTDEEIDEYIRNSLHTANALTGTCKMGTGRGAV
	VGPDLRVIGVNGVRVADSSVFPCIPGGQTATPTVMIADRAAVFVR

[a]The exact cleavage site of the putative signal peptides to form mature FAP enzymes was estimated according to UniProt. [b]No chloroplast or mitochondrial targeting sequence identified. Red = mutation to generate a N-terminal *Nco*I restriction site; Orange bold = location of the G462V mutation.

Table S2. Oligonucleotide and other DNA sequences in *E. coli* and *Halomonas*.

Protein	DNA sequence
pPorin 102 promoter	TTGCGTCCTGATCGTAGTGCGTATAGAGTTTGAGAC*TTTACTAGAGAAAGAGGAGAAATACTAG*
pPorin 69 promoter	TTGCGTGCTCATTGGCCAATGTATAGAGTTTGAGAC*TTTACTAGAGAAAGAGGAGAAATACTAG*
Mutagenesis in E. coli	
$CvFAP_{G462V}$	5′-GCACTGGATCCGGAT*GTT*GTTAGCACCTATGTG-3′
	5′-CACATAGGTGCTAAC*AAC*ATCCGGATCCAGTGC-3′
$CvFAP_{G462I}$	5′-GATCCGGATATTGTTAGCACCTATG-3′
	5′-CAGTGCCATACCAGGAACAAAAC-3′
$CvFAP_{G462F}$	5′-GATCCGGATTTTGTTAGCACC-3′
	5′-CAGTGCCATACCAGGAACAAAAC-3′
$CvFAP_{G462A}$	5′-GCGGTTAGCACCTATGTGCGTTTTG-3′
	5′-ATCCGGATCCAGTGCCATAC-3′
$CvFAP_{G462H}$	5′-CAGTGCCATACCAGGAACAAAACG-3′
	5′-CAGTGCCATACCAGGAACAAAAC-3′
$CvFAP_{G462L}$	5′-GATCCGGATCACGTTAGCACCTATG-3′
	5′-GATCCGGATCTGGTTAGCACCTATG-3′
$CvFAP_{G462C}$	5′-GATCCGGATTGTGTTAGCACCTATG-3′
	5′-GATCCGGATTGGGTTAGCACCTATG-3′
$CvFAP_{G462W}$	5′-GATCCGGATTATGTTAGCACCTATG-3′
	5′-GATCCGGATAACGTTAGCACCTATG-3′
$CvFAP_{G462Y}$	5′-GATCCGGATTATGTTAGCACCTATG-3′
	5′-CAGTGCCATACCAGGAACAAAAC-3′
$CvFAP_{G462N}$	5′-GATCCGGATAACGTTAGCACCTATG-3′
	5′-CAGTGCCATACCAGGAACAAAACG-3′
$CvFAP_{G455F}$	5′-GTTTTGTTCCTTTTATGGCACTGGATCC-3′
	5′-GAACTTGCAGATCCGGCAG-3′
$CvFAP_{G455I}$	5′-GTTTTGTTCCTATTATGGCACTGGATCC-3′
	5′-GAACTTGCAGATCCGGCAG-3′
$CvFAP_{G455V}$	5′-GTTTTGTTCCTGTTATGGCACTGGATCC-3′
	5′-GAACTTGCAGATCCGGCAG-3′
$CvFAP_{G455W}$	5′-GTTTTGTTCCTTGGATGGCACTGGATC-3′
	5′-GAACTTGCAGATCCGGCAG-3′
$CvFAP_{G455L}$	5′-TTTTGTTCCTCTGATGGCACTGGATCC-3′
	5′-CGAACTTGCAGATCCGGC-3′
$CvFAP_{Y466W}$	5′-GTGTTAGCACCTGGGTGCGTTTTG-3′
	5′-CATCCGGATCCAGTGCCATAC-3′
$CvFAP_{V453L}$	5′-CAAGTTCGTTTTCTGCCTGGTATGGCAC-3′
	5′-CAGATCCGGCAGTGCCTG-3′
$CvFAP_{V453W}$	5′-CAAGTTCGTTTTTGGCCTGGTATGGCAC-3′
	5′-CAGATCCGGCAGTGCCTG-3′
$CvFAP_{V453F}$	5′-CAAGTTCGTTTTTTTCCTGGTATGGCAC-3′
	5′-CAGATCCGGCAGTGCCTG-3′
$CvFAP_{V453I}$	5′-CAAGTTCGTTTTATTCCTGGTATGGCAC-3′
	5′-CAGATCCGGCAGTGCCTG-3′
$CvFAP_{T484I}$	5′-GCCTGAAATGGCCGAGCGGTATTDHMATGCAGCTGATTGCATGT-3′
	5′-CCTGGCTCTGAAATTTGGCAAAACG-3′
$CvFAP_{T484L}$	5′-GCCTGAAATGGCCGAGCGGTATTDHMATGCAGCTGATTGCATGT-3′
	5′-CCTGGCTCTGAAATTTGGCAAAACG-3′
$CvFAP_{T484E}$	5′-GCCTGAAATGGCCGAGCGGTATTDHMATGCAGCTGATTGCATGT-3′
	5′-CCTGGCTCTGAAATTTGGCAAAACG-3′
$CvFAP_{T484A}$	5′-GCCTGAAATGGCCGAGCGGTATTDHMATGCAGCTGATTGCATGT-3′
	5′-CCTGGCTCTGAAATTTGGCAAAACG-3′

$CvFAP_{A457L}$	5′-GTTCGTTTTGTTCCTGGTATGNTTCTGGATCCGGATGGTGTTAGC-3′
	5′-GCTAACACCATCCGGATCCAGAANCATACCAGGAACAAAACGAAC-3′
$CvFAP_{A457V}$	5′-GTTCGTTTTGTTCCTGGTATGNTTCTGGATCCGGATGGTGTTAGC-3′
	5′-GCTAACACCATCCGGATCCAGAANCATACCAGGAACAAAACGAAC-3′
$CvFAP_{A457I}$	5′-GTTCGTTTTGTTCCTGGTATGNTTCTGGATCCGGATGGTGTTAGC-3′
	5′-GCTAACACCATCCGGATCCAGAANCATACCAGGAACAAAACGAAC-3′
$CvFAP_{A457F}$	5′-GTTCGTTTTGTTCCTGGTATGNTTCTGGATCCGGATGGTGTTAGC-3′
	5′-GCTAACACCATCCGGATCCAGAANCATACCAGGAACAAAACGAAC-3′
Assembly of pHal1-FAP_{WT}	
Vector opening	5′-TGCCACCGCTGAGCAATAAAA-3′
	5′-CATCTAGTATTTCTCCTCTTTCTCTAGTA-3′
Insert generation	5′-GAGAAATACTAGATGGCCAGCGCAGTTGAAGATATT-3′
	5′-TGCTCAGCGGTGGCATTATGCTGCAACGGTTGCCG-3′
Generation of FAP_{G462V} in pET21b	
Vector opening	5′-CTGAAAGGAGGAACTATATCCGGATTG-3′
	5′-AGTTCCTCCTTTCAGCTCTACGCCGGACGCATCGT-3′
Assembly of pTrc-ilvE-Hpad-KcdA-$CvFAP_{G462I}$ in pBbE1k	
Vector opening	5′-TTCTTTATCCTCCTTCTTAAAAGATCTTTTGAATTCTGAAATTGTTATCCGCTC-3′
	5′-GGATCCAAACTCGAGTAAGGATCTCC-3′
CvFAP PCR	5′-CAGAACAAATAAAGGAGGATAAAGAAATGGCCAGCGCAGTTGAAG-3′
	5′-CCTTACTCGAGTTTGGATCCTTATGCTGCAACGGTTGCCGG-3′
ilvE PCR	5′-TTAAGAAGGAGGATAAAGAAATGACCACCAAAAAAGCCGATTACATTTGG-3′
	5′-TTCTTTATCCTCCTTCACTCGAGCTGATTAACCTGATCCAG-3′
Hpad PCR	5′-CAGCTCGAGTGAAGGAGGATAAAGAAATGGACTTTCATCATCTGGCCTATTGG-3′
	5′CATTATACGAGCCGGATGATTAATTGTCAATCATGCTTCCAGGCTAATCCAAATGGTTTTCAG-3′
KdcA PCR	5′-ATCTTTTAAGAAGGAGGATAAAGAAATGTATACCGTGGGTGATTATCTGC-3′
	5′-GGCCATTTCTTTATCCTCCTTTATTTGTTCTGTTCCGCAAACAGTTTGC-3′
OEP	5′-GACACCATCGAATGGTGCAAAACCTTTCGCGG-3′
	5′-GGCCATTTCTTTATCCTCCTTTATTTGTTCTGTTCCGCAAACAGTTTGC-3′

[a]Italics = Shine-Delgarno sequence.

Table S3. Prefix and suffix oligonucleotides used for DNA assembly.

Assembly	Prefix linker	Plasmid	Suffix linker
Plasmid: pIY918 or pJET-Ptrc-Tes4-CvFAPG462V			
	LRBS1-4P	pIY840	LRBS2-4S
1	LRBS2-4P	pIY882	1S
	1P	pIY345[2]	LRBS1-4S
Plasmid: pIY906 or pJET-Pcoa-Tes4-CvFAPG462V			
	LRBS1-4P	pIY840	LRBS2-4S
2	LRBS2-4P	pIY882	1S
	1P	pIY417[2]	LRBS1-4S
Plasmid: pIY894 or pJET-Ptrc-CvFAPG462V			
3	LRBS1-4P	pIY882	1S
	1P	pIY345	LRBS1-4S
Plasmid: pIY845 or pJET-Pcoa-Tes4			
4	LRBS1-4P	pIY840	1S
	1P	pIY417[2]	LRBS1-4S

Plasmids pIY345 and pIY417 are described in Yunus, I. S. and Jones, P. R. (2018).[1]

Table S4. Prefix and suffix oligonucleotide linkers.

Adapter Name	Sequence (5' to 3')	Linker Name	Sequence (5' to 3')	Linker
Prefix linkers				
1P-A	TTTATTGAACTA	1P-L	GGACTAGTTCAATAAATACCCTCT GACTGTCTCGGAG	1P
LRBS1-4P-A	ATCACAAGGAGGTA	LRBS1-4P-L	GGACTACCTCCTTGTGATTTACAA CTGATACTTACCTGA	LRBS1-4P
LRBS2-4P-A	ATCACAAGGAGGTA	LRBS2-4P-L	GGACTACCTCCTTGTGATTTTCTG CTACCCTTATCTCAG	LRBS2-4P
Suffix linkers				
1S-A	TGTCGTAAGTAA	1S-L	CTCGTTACTTACGACACTCCGAGA CAGTCAGAGGGTA	1S
LRBS1-4S-A	GACGGTGTTCAA	LRBS1-4S-L	CTCGTTGAACACCGTCTCAGGTAA GTATCAGTTGTAA	LRBS1-4S
LRBS2-4S-A	CCAATAGTAACA	LRBS2-4S-L	CTCGTGTTACTATTGGCTGAGATA AGGGTAGCAGAAA	LRBS2-4S

Table S5. Screening of putative FAP homologues in *E. coli*.

Homologue	Soluble expression	Propane production (mg/L culture)
CvFAP	High	0.336 ± 0.021
CrFAP	High	0.495 ± 0.073
GpFAP	Medium	0.164 ± 0.016
CcFAP	Low	0.001 ± 0.002
ChFAP	Low	0.009 ± 0.002
CsFAP	Medium	0.131 ± 0.021
PtFAP	Low	ND
CmFAP	Low	0.002 ± 0.004

Cultures were grown in LB medium containing kanamycin (30 μg/mL) at 37 °C at 200 rpm until 0.2 OD_{600nm} followed by temperature reduction to 25°C. Recombinant protein expression was induced at 0.6-0.8 OD_{600nm} with 0.5 mM IPTG and the cultures were incubated overnight at 17°C. Cells were lysed by sonication and centrifuged (48000 × *g*, 4°C, 30 min). 400 μM butyric acid was added to 1 ml clarified lysate and sealed in 4 ml glass vials with gas-tight caps with septa. The reactions were incubated at 30 °C for 24 h at 200 rpm under a blue light LED. Headspace gas was analyzed for propane content using a Micro GC with an Al_2O_3/KCl column. Further experiments focused on CvFAP due to its high solubility and availability of crystal structure to inform rational engineering of the enzyme. Error bars represent one standard deviation of the data from technical replicates (n=3). ND = none detected.

Table S6. Propane production by $CvFAP_{WT}$ and variants in *E. coli*.

Variant	Propane production (mg/L culture)	Relative activity[a] (mg/L culture, normalised)
WT	0.67 ± 0.24	0.67 ± 0.24
V453F	0.95 ± 0.14	0.74 ± 0.11
V453I	1.81 ± 0.55	1.51 ± 0.45
V453L	0.33 ± 0.18	0.32 ± 0.17
V453W	1.25 ± 0.13	1.47 ± 0.16
G455F	0.29 ± 0.07	0.25 ± 0.06
G455I	0.08 ± 0.01	0.15 ± 0.02
G455V	0.05 ± 0.00	0.06 ± 0.00
G455W	0.25 ± 0.16	0.33 ± 0.21
G455L	0.08 ± 0.10	0.19 ± 0.24
A457F	0.02 ± 0.02	-
A457I	0.03 ± 0.10	0.03 ± 0.11
A457L	0.04 ± 0.08	0.05 ± 0.12
A457V	0.07 ± 0.15	0.07 ± 0.16
G462A	7.14 ± 1.09	16.85 ± 2.58
G462C	3.94 ± 2.38	5.90 ± 3.57
G462F	7.00 ± 0.38	9.36 ± 0.51
G462H	0.04 ± 0.02	0.04 ± 0.02
G462I	10.77 ± 1.19	14.75 ± 1.63
G462L	0.02 ± 0.01	-
G462N	0.53 ± 0.08	0.83 ± 0.12
G462V	3.41 ± 2.99	3.25 ± 2.85
G462W	0.61 ± 0.19	0.57 ± 0.18
G462Y	0.83 ± 0.46	1.62 ± 0.91
Y466W	0.23 ± 0.08	0.48 ± 0.15
T484A	0.03 ± 0.03	0.02 ± 0.02
T484E	0.01 ± 0.01	0.02 ± 0.01
T484I	0.00 ± 0.01	0.01 ± 0.01
T484L	0.03 ± 0.05	0.04 ± 0.05

5 ml overnight cultures (LB medium containing 30 μg/mL kanamycin) were started from 3 individual bacterial colonies on a transformation plate of each CvFAP variant in pETM11 (biological replicates). Cultures (20 mL) were grown in LB medium at 37 ºC until OD600nm = ~1.0. Recombinant protein expression was induced with IPTG (0.1 mM) and cells were grown for 1 hour more at 30 ºC. 1 ml of culture was transferred to a 4 ml glass screw-top vial and 10 mM butyric acid was added. Vials were sealed and incubated at 30 ºC for 16-18 h at 200 rpm, illuminated with a blue LED array. Headspace gas was analyzed for gaseous hydrocarbon content using a Micro GC. Normalised data were calculated by dividing the propane yields (mg/L culture) by the relative protein concentration compared to the wild type (WT) enzyme (**Fig. S2**). Error bars represent one standard deviation of the data using biological triplicates (n=3). [a]Lysates of A457I and G462L did not show visible bands on SDS PAGE. Discussion on the statistical analysis of this data and **Table S10** is found in Supplementary **Note S2**.

Table S7. Molecular docking simulations of CvPAS wild-type and variants with butyrate and palmitate.

Variant	ΔΔG (kcal/mol)		K_d	
	Butyrate	Palmitate	Butyrate	Palmitate
WT	0.00	0.00	1.00	1.00
G462V	-0.20	2.20	0.72	40.1
G462I	-0.20	2.00	0.72	28.6
G462L	-0.20	0.00	0.72	1.00
V453I	-0.10	0.20	0.85	1.40
G455I	-0.20	-0.40	0.72	0.51
Y466W	0.10	1.30	1.18	8.85
T484I	0.00	0.40	1.00	1.96
A457V	-0.10	0.90	0.85	4.53

Molecular docking simulations were performed using Autodock Vina and the wild-type crystal structure of CvFAP.[3] Values of the predicted binding affinity are given relative to the WT ($\Delta\Delta G = \Delta G_{variant} - \Delta G_{WT}$) and dissociation constants are normalized against the values for WT ($K_d = K_{d,variant} / K_{d,WT}$).

Table S8. Propane production by $CvFAP_{WT}$ and variants with pH control.

Variant	Propane production (mg/L culture)
$CvFAP_{WT}$	17.07 ± 1.56
$CvFAP_{G462I}$	62.19 ± 2.47
$CvFAP_{G462V}$	34.19 ± 2.75

5 ml overnight cultures (LB medium containing 30 μg/ml kanamycin) were started from 3 individual bacterial colonies on a transformation plate of each CvFAP variant in the pETM11 vector (biological replicates). 20 ml cultures were inoculated the next morning with 1% of the overnight culture and grown at 37°C with shaking at 180 rpm until OD600nm = ~1.0. The cells were inoculated with 0.1 mM IPTG and grown for 1 hour more at 30°C with shaking at 180 rpm. 1 ml of culture was transferred to a glass screw-top vial (4 ml) and 50 mM butyric acid was added (1M stock in water, pH 6.8). 50 mM K_2HPO_4 was added to control pH of reactions. Vials were sealed with gas-tight caps with septa and incubated overnight under a blue light LED array at 30°C with shaking at 200 rpm. Propane analysis was done by manual injection of 2 ml samples and quantified using a Micro GC. Errors represent one standard deviation of the data using three biological and technical replicates (n=9). Discussion on the statistical analysis of this data and **Table S8** is found in Supplementary **Note S2**.

Table S9. Hydrocarbon production by variant CvFAP with short-chain fatty acids.

	Substrate acid				
	Butyric	Isobutyric	Valeric	2-MB	Isovaleric
Variant	Propane (mg/L culture)		Butane (mg/L culture)		Isobutane (mg/L culture)
WT	7.0 ± 0.6	6.1 ± 2.4	17.7 ± 1.9	7.1 ± 1.4	5.6 ± 0.3
G462A	17.6 ± 0.7	5.0 ± 1.2	33.5 ± 6.5	50.0 ± 11.4	30.2 ± 3.9
G462I	43.8 ± 3.1	36.9 ± 5.4	47.1 ± 7.8	95.4 ± 5.8	86.8 ± 10.8
G462F	31.2 ± 0.7	31.4 ± 3.3	27.7 ± 0.8	38.5 ± 10.9	28.6 ± 4.0
G462V	24.5 ± 5.0	24.3 ± 1.6	21.9 ± 0.7	12.2 ± 2.1	17.4 ± 2.0

Cultures of *E. coli* BL21(DE3) ΔyqhD ΔyjgB with pETM11-CvFAP variants (3 biological replicates) in LB medium containing kanamycin (50 μg/mL) were inoculated at 1% volume from overnight starter cultures and grown further at 37 ºC to 0.6-0.8 OD_{600} Recombinant protein expression was induced with IPTG (0.1 mM) and cultures were supplemented with different short-chain fatty acids (10 mM). Triplicate 1 mL aliquots were sealed into 5 mL glass vials and incubated at 30 ºC for 16-18 h at 200 rpm, illuminated continuously under a blue LED panel. Headspace gas was analysed for propane content using a Micro GC (100 ms injection) with an Al_2O_3/KCl column. Errors represent one standard deviation of biological triplicates (n=3). WT = wild type; 2-MB = 2-methylbutyric acid.

Table S10. Effect of VFA blends on gaseous hydrocarbon production by $CvFAP_{WT}$.

Butyric Acid (%)	Valeric acid (%)	Propane (mg/L culture)	Butane (mg/L culture)
0	0	0.6 ± 0.06	0.03 ± 0.00
0	100	0.21 ± 0.01	17.13 ± 0.31
20	80	3.62 ± 0.13	13.74 ± 0.42
30	70	5.76 ± 0.04	13.15 ± 0.03
35	65	6.43 ± 0.25	11.87 ± 0.5
40	60	7.39 ± 0.22	10.99 ± 0.07
50	50	8.75 ± 1.04	8.37 ± 0.91
60	40	11.67 ± 0.66	7.41 ± 0.29
70	30	11.96 ± 1.32	5.02 ± 0.59
80	20	14.04 ± 0.22	3.72 ± 0.05
90	10	17.29 ± 0.53	1.95 ± 0.04
92	8	17.56 ± 0.31	1.57 ± 0.05
95	5	17.10 ± 0.24	0.99 ± 0.02
100	0	19.32 ± 1.55	0.00 ± 0.00

Cultures in LB were grown and induced with IPTG (0.1 mM) as already described (**Table S10**), then supplemented with butyric/valeric acid mixtures (10 mM total). Triplicate 1 mL aliquots were sealed into 5 mL glass vials and incubated at 30 ºC for 16-18 h at 200 rpm, illuminated with a blue LED panel. Headspace gas was analyzed for gaseous hydrocarbon content using a Micro GC. Errors represent one standard deviation of the data from biological duplicates (n=2).

Table S11. Effect of valine supplementation on hydrocarbon production by $CvFAP_{G462I}$.

Valine (mg/mL)	Propane (mg/L culture)	Isobutane (mg/L culture)	Butane (mg/L culture)
0	6.33 ± 0.31	30.13 ± 1.45	7.37 ± 0.33
1	22.16 ± 1.57	28.44 ± 1.46	7.15 ± 0.34
2	39.07 ± 0.64	28.07 ± 1.10	7.23 ± 0.26
4	51.26 ± 5.96	20.76 ± 2.88	5.43 ± 0.75
8	73.02 ± 5.55	17.39 ± 1.28	4.85 ± 0.30
10	56.44 ± 2.96	9.69 ± 0.45	2.84 ± 0.12
15	75.71 ± 3.77	9.48 ± 0.44	2.86 ± 0.14
20	93.95 ± 3.69	9.24 ± 0.52	3.00 ± 0.21
25	81.90 ± 4.46	6.61 ± 0.38	2.25 ± 0.12
30	109.72 ± 6.34	5.83 ± 0.37	2.10 ± 0.14

Cultures (20 mL; 3 biological replicates) were grown in LB medium containing kanamycin (50 μg/mL) at 37 ºC until OD 600 nm reached ~ 0.6-0.8. Recombinant protein expression was induced with IPTG (0.1 mM) followed by culture supplementation with valine (0-35 mg/L) after 1 h at 30 ºC. Triplicate aliquots (1 mL) of each culture were sealed into 4 mL glass vials and incubated at 30 ºC for 16-18 h at 200 rpm, illuminated with a blue LED panel. Headspace gas was analyzed for hydrocarbon content using a Micro GC. Errors represent one standard deviation of the data from biological and technical triplicates (n=9).

Table S12. Propane production by CvFAP$_{G462V}$ in *Halomona*s.

Butyric acid (mM)	Additive	Propane (mg/L culture)
0	None	0.9 ± 0.1
10	None	54.9 ± 1.4
20	None	96.7 ± 1.6
30	None	117.2 ± 15.4
40	None	119.7 ± 15.3
50	None	138.4 ± 6.32
60	None	133.7 ± 2.25
80	None	157.1 ± 17.14
100	None	102.2 ± 7.0
57.8 ± 8.7	(*Synechocystis*)[a]	25.3 ± 5.8

Cultures of *Halomonas* TQ10-MmP1 containing pHal2-CvFAP$_{G462V}$ were grown in YTN6 medium (yeast extract 5 g/L, tryptone 10 g/L, NaCl 60 g/L, pH 9.0/NaOH) containing spectinomycin (50 μg/mL) were inoculated from overnight starter cultures at 1% volume and grown at 37 ºC at 180 rpm to 1.0–1.2 OD_{600}. Recombinant protein expression was induced with IPTG (0.1 mM). Cultures were adjusted to pH 6.8 by combined addition of KH_2PO_4 (50 mM) and butyrate (1-25 mM)*. Triplicate 1 mL aliquots were sealed into 5 mL glass vials and incubated at 30 ºC for 16-18 h at 180 rpm, illuminated continuously under a blue LED array. Headspace gas was analyzed for propane content using a Micro GC (100 ms injection) with an Al_2O_3/KCl column. Error bars represent one standard deviation of the data from technical triplicates (n=3). Optimal culture pH for propane production by CvFAP in *Halomonas* was pH 6.5-7.0. It was therefore necessary to adjust the pH of the butyrate solution accordingly prior to mixing with the culture.
[a]*Synechocystis* cell culture in BG11 medium containing ~50 mM butyric acid produced during growth, as measured by HPLC, were lysed osmotically by 1:1 addition to 2 x LB60 medium and subsequently used for growth and propane production of *Halomonas* over-expressing CvFAP$_{G462V}$. The addition of the lysed *Synechocystis* cellular material reduced the propane titre relative to pure butyric acid addition 138.4 mg/L from 50 mM pure butyrate vs 25.3 mg/L.

Supplementary Notes

S1. Techno-Economic Analysis (TEA) and Carbon Footprint Analysis.[4-7]

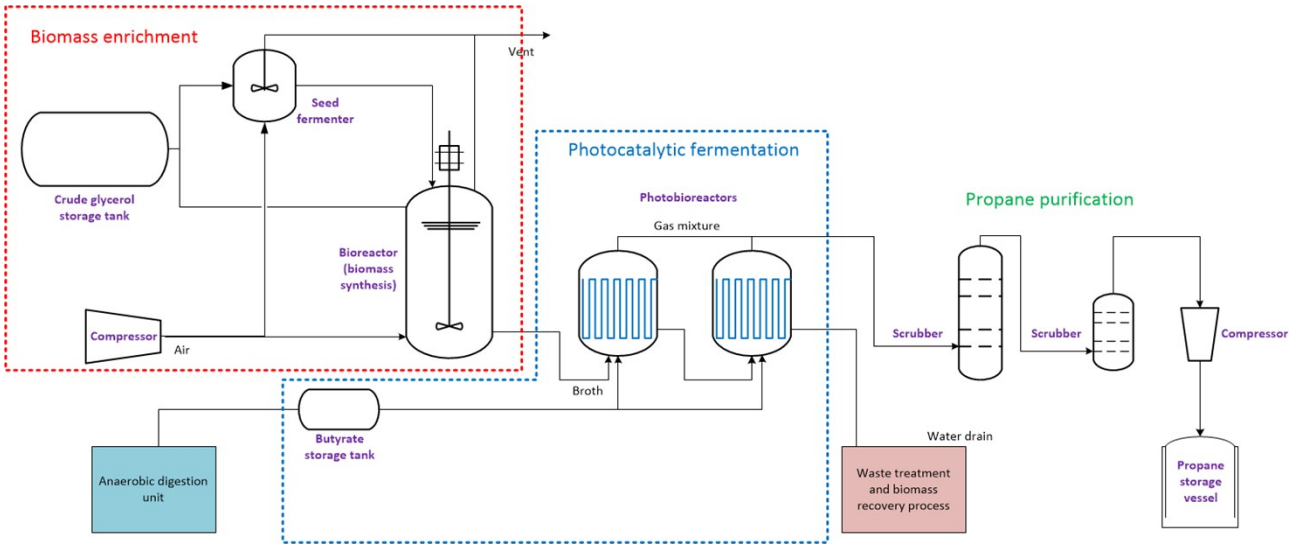

Fig. S9. Process flow diagram of a conceptual continuous photocatalytic bio-propane process

As presented in the main manuscript, a bioprocess has been developed based on a recombinant *Halomonas* strain (*Halomonas* XV12), which is capable of using glycerol and butyrate as the main carbon sources to synthesise biomass, propane and chemicals. A preliminary techno-economic analysis (TEA) is conducted for the said bioprocess (**Fig. S9**) in order to provide projected economics and establish benchmarks to assess the state of technology based on current research performance. The objective in this TEA is to estimate the production costs for the main unit operations for such a plant at pilot scale (base case: 3×1 m^3 reactor working volume). Based on the operating costs and an estimated fixed capital cost of £500,000 (offered by a leading commercial supplier), we proceeded to estimate the minimum propane selling price (MPSP), namely the price at which propane must be sold in order to generate a net present value of 0 for a specified return by the end of the plant life.

Table S13. General design basis for base case propane manufacturing process

Parameter (utility)	**Value**	**Sources**
Electricity price (£/kWh) (typical price for middle to large scale process in the industry)	0.125	Industrial energy price statistics (gov.uk)
Electricity price (£/kWh) (onshore wind turbine)	0.06	Business Electricity Prices
Crude glycerol unit price ($/kg) (composition, 80% glycerol)	0.115	Alibaba
Process water price (£/m3)	1.361	Thames Water Utilities Ltd
Wastewater price (£/m3)	0.892	Thames Water Utilities Ltd
Compressor specific power (kW/(m^3/h))	0.083	100 psia delivery, air compressor
Parameter (material)	**Value**	**Sources**
Ammonium phosphate price ($/kg) (industrial grade)	0.150	(Alibaba, RPI, ICIS)
NaCl price ($/kg)	0.04	
Other medium ingredients, including IPTG ($/$m^3$ of medium)	126.8	
Other medium ingredients, excluding IPTG ($/$m^3$ of medium)	4.37	

Crude glycerol unit price ($/kg) (composition: 80% glycerol,14% water, 6% NaCl)	0.115	
NaCl price ($/kg)	0.04	
Parameter (process)	**Value**	**Sources**
NaCl concentration in sea water (g/l)	35	Assumed
Fermenter residence time (h)	24	
Fermenter working volume (pilot scale) (l)	1000	
Compressor specific power (kW/(m^3/h))	0.083	

Conceptual design

TEA starts with the conceptual design of the proposed process. The process flow diagram for a pilot-scale, continuous bioprocess is presented in **Fig. S9**, which includes five unit operations:

1) Biomass enrichment
2) Anaerobic digestion
3) Photo-catalytic fermentation
4) Waste treatment and biomass recovery
5) Propane purification

TEA simulation was performed in MATLAB 2019a and MS Excel. The general TEA information regarding utility prices, material purchase and selling price are summarised in **Table S13**. Process descriptions and process-specific TEA assumptions are detailed in the following sections.

Biomass enrichment

Crude glycerol is used as the carbon source for the *Halomonas* strain. Carbon sources and nutrients are continuously fed into an aerobic fermenter along with other nutrients. A CSTR is used as it is good at handling viscous fermentation broths and providing mixing to ensure efficient mass and energy transfer. This unit operation purely focuses on the enrichment of *Halomonas* biomass, as high cell density is crucial to achieving high propane productivity in the subsequent step. The fermenter model was simulated under the assumption that two simultaneous biochemical reactions take place: biomass synthesis (Eq. (1)) and respiration (Eq. (2)).

$$C_3H_8O_3 + 0.883O_2 \rightarrow 3CH_{1.41}O_{0.96} + 1.885H_2O \quad (1)$$

$$C_3H_8O_3 + 3.5O_2 \rightarrow 3CO_2 + 4H_2O \quad (2)$$

No propane is produced at this stage due to the absence of light source. The assumptions regarding biomass enrichment are summarised in **Table S14**.

Table S14. TEA assumptions for biomass enrichment unit

Parameter	**Value**
Dry cell density (gCell/l)	10
Temperature (°C)	30
Fermenter residence time (h)	24
Fermenter working volume (pilot scale) (l)	1000
Specific power input (P/V) (W/L)	1.5
Halomonas elemental formula [8]	$CH_{1.41}N_{0.39}O_{0.96}P_{0.18}$
Carbon split ratio between respiration and biomass synthesis	0.5
Compressor specific power (kW/(m^3/h))	0.083
Aeration rate (vvm)	1

Anaerobic digestion (AD)

Butyric acid utilised by the *Halomonas* strain to produce propane is sourced from an anaerobic digestion (AD) process. AD is a versatile valorisation method for organic waste materials, typically used to produce biogas (mainly methane).[7] Volatile fatty acids (VFAs), including butyric acid, are intermediates in the methane formation pathway of conventional AD processes, which means they can be produced in a similar manner to biogas in an anaerobic digestor.

Food wastage is an increasingly recognised global issue, which has put a heavy price on our economy, health and environment. According to the Food and Agriculture Organisation (FAO), approximately 1.3 billion tonnes of food is wasted.[9] In the UK, the annual amount of house food waste is over 7 million tonnes,[10] of which around 10% can be collected separately by local authorities owing to the waste collection practices enforced by the UK government. This has promoted numerous opportunities for utilising food waste for VFAs production. Food waste has a great potential as a VFA fermentation substrate due to its high VFA yield (i.e. up to 0.43 gVFA/g substrate).[7] VFAs produced from AD is primarily a mixture of acetate, propionic, butyric, caproic and valeric acids, while the exact composition is subject to the type of organic matters, fermentation conditions and microbial cultures used.[11] It has been shown that by selectively feeding starch-rich food waste and employing strains such as *Clostridiales* as microbial producers, butyrate accumulation can be significantly enhanced.[12] In a study where kitchen food waste is used as the feedstock, an AD process inoculated with the digestion sludge from a local wastewater treatment process can yield 41 g/L of VFAs in 55 hours.[13] Butyrate content in VFAs varies between 19-51% depending on the oil and salt content of the food waste. The butyrate and other VFAs produced need to be separated and concentrated from the digestate suspension by means of filtration and reverse osmosis before being feed to downstream processes.

Due to the lack of examples of commercial production of VFAs by AD and available TEA data, we based the calculation of butyrate production cost partially on a recent feasibility study of a biogas generating AD process in France.[14] Slurry from the digester is dewatered (typically in a centrifuge dewatering system). The anaerobic digestion liquor containing VFA is sent to the following photocatalytic fermentation unit. The assumptions regarding AD are detailed in **Table S15**.

Table S15. TEA assumptions for the production of butyrate through anaerobic digestion

AD parameters and conditions	**Description/value**
AD process type	CSTR
Feed type	Food waste, preferably rich in starch
Food waste density (kg/m^3)	1200
Water content of food waste (wt %)	70
Butyrate content in VFA	40%
VFA yield	200 gVFAs/kg feed
Hydraulic retention time (hours)	55
Final butyrate concentration (kg/m^3)	20
Operating cost breakdown	**$/kg butyrate**
Water	0.002
Gasoil	0.015
Air treatment	0.017
Water treatment	0.015
Others	0.029
Refuse to landfill	0.256

Hazardous water treatment	0.043
Separation	0.007
Total OPEX	0.355

Photocatalytic fermentation

During photocatalytic fermentation, culture broth containing sufficient *Halomonas* biomass produces propane from butyric acid in the presence of blue light source (wavelength: 450 nm to 470 nm). This unit operation consists of two LED-lit, flat panel photobioreactors (PBRs) connected in series. Illumination specifications and requirements were first measured in a 400 ml lab-scale flat panel PBR with 50 mm light path (**Table S16**). The data were then extrapolated to predict the illumination requirements in larger-scale PBRs.

Table S16. Illumination parameters in photobioreactors

Illumination parameters (Small PBR)	**Value**
Optimal incident light intensity (μmol photon/m^2-s), determined experimentally	1650
Light wavelength (nm)	465 (blue)
Incident light intensity (W/m^2)	425
Light path length (mm)	50
Test absorbance (OD465). OD465 was measured by photospectrometer (light path length=10mm)	1
Correlations between absorbance (OD465) and biomass concentration *X (g/l)*	$OD = 4.063X\ (X \leq 0.2)$ $OD = 1.237X^3 - 3.8942X^2 + 4.5063X + 0.1$ $OD = 0.3281\ln(X) + 1.968\ (X \geq 1)$
Estimated average light intensity of illuminated space (μmol photon/m^2-s),	216
Typical luminous efficiency of LED	0.48
Illumination parameters (Pilot-scale PBR)	**Value**
Light path (mm)	150

According to experimental results, the optimal propane productivity in the small-scale PBR is achieved when incident light intensity equals 1650 microeinsteins (where the culture absorbance at 465nm wavelength equals 1). Light intensity I along the light path can be expressed using Beer-Lambert Law (Eq. (3)):

$$log_{10}\left(\frac{I_0}{I}\right) = absorbance(OD465) = \varepsilon X l \quad (3)$$

Where I_0 is the incident light intensity, X stands for biomass concentration, l stands of the light path length and ε stands for the absorptivity. Due to the light scattering effect by cells, the absorptivity of cell culture is not constant, but rather a function of biomass concentration (namely ε=f(X)). In sufficiently mixed cell culture, the average light intensity of illuminated space is given by Eq. (4):

$$I_{average} = \frac{1}{l}\int_{l=0}^{l=l} I dl = \frac{I_0}{l}\int_{l=0}^{l=l} 10^{-\varepsilon X l} dl \quad (4)$$

The illumination area for the pilot-scale PBRs can be adjusted accordingly to provide the same level of average light intensity as in the lab-scale PBR.

The design parameters related to propane production are summarised in **Table S17**. Digestate containing butyrate from the upstream AD process is fed into PBRs after being adjusted to appropriate pH. In the first PBR, the butyrate concentration is maintained at 50 mM, which is optimal for the propane synthesis. In the second PBR, conversion of butyrate to propane continues, but at a slower rate due to having lower butyrate concentration. The influence of reduced substrate concentration on propane synthesis is taken into account with a Michaelis-Menten type kinetic equation (**Table E**). According to experimental observation, 75% of the carbon in butyrate is converted to propane, with the rest converted to CO_2. Therefore, the gas stream from PBRs is a mixture of propane, carbon dioxide and a small amount of moisture.

Table S17. Propane production parameters and assumptions

Process parameters	**Value**
Butyrate concentration in reactor 1 (mM)	50
Maximum specific propane production rate q_{max} (mg/gCell-h)	28.8
Kinetic equation for propane production	$\frac{dP}{dt} = x_v q_{max} \frac{S}{S+E} k$ where dP/dt = production rate of propane (g/l-h) x_v = cell density (g/l) q_{max} = max specific propane production rate (see above) S = concentration of butyrate (mM) k = 1.11, constant
Butyrate to propane yield (w/w)	3
Temperature (°C)	30
Reactor 1&2 working volume (L)	1000
Specific power input (P/V) (W/L)	1.5

It should be noted that AD digestate is a complex medium consisting of not only butyrate but also other compounds that may interfere with propane synthesis in PBRs. In the present base case, we benchmark the process performance by neglecting the potential side effects of impurities in butyrate feed on the metabolic activity of cells. Nonetheless, for future studies, such effects must be carefully taken into account as a relevant factor for determining whether the AD-derived butyrate is the optimal substrate for propane synthesis.

Biomass and waste recovery

Waste broth discharged from PBRs contains unreacted organic nutrients (glycerol, butyrate etc), salts and genetically modified biomass that are worthy of recovery. First of all, microbial biomass contains different levels of amino acids, fatty acids, vitamin, etc, which make it a potential source for use in aquaculture feed supplement.[15, 16] Secondly, *Halomonas* sp. accumulates ectoine in the cytoplasm to help maintain conformation and activity of proteins when living in halophilic environments. According to our experiments, *Halomonas* XV21 produces approximately 0.15-0.2 g of ectoine per g of dry cell mass. Ectoine is a compound of relatively high commercial value, typically used as active ingredients in skincare products and enzyme stabiliser.[17]

Recovering organic matters from the waste broth is an important means to strengthen the economic potential of this process, meanwhile reducing the generation of wastes. To maximise the recovery of usable constituents in the waste broth, the following additional steps are considered:

1) Separation and concentration of biomass from culture broth via microfiltration and centrifugation.
2) Subject the cell concentrate to osmotic down shock by dilution with water, forcing the release of ectoine. This step is known as "bacterial milking".[18]
3) Released ectoine is further purified by cross-flow filtration, chromatography and crystallisation and drying,[19] resulting in ectoine powder with high purity (>98%)
4) Desalting and drying of biomass.
5) Milling of biomass and pelletisation.
6) Decontamination and disposal of biological waste through specialised contractors.

Assumptions regarding biomass recovery and ectoine extraction are summarised in **Table S18**. Economic parameters regarding the production of aquafeed are taken from a TEA for single-cell protein process conducted by Litchfield.[20] On the other hand, despite that "bacterial milking" technique has been invented for more than two decades, there was no published information for extraction and purification of ectoine in from large scale production processes to allow for accurate estimation of the production cost of ectoine. To compensate for known underestimation, ectoine is only sold for half of its market price in our case study.

Table S18. TEA assumptions for aquafeed and ectoine production

Parameter	**Value**
Electricity	2.06kWh/ kg DCW processed
Steam requirement	2.3kg/kg DCW processed
Conversion of DCW to fishmeal	90% wt
Ectoine content	0.15g/gDCW
Ectoine recovery	60%
Ectoine price ($/kg)	1000*50%
Aquafeed ($/kg)	1.5
Waste treatment ($/$m^3$ broth)	1.18

Propane purification (99% minimum purity)

The fermentation gas from PBRs is a mixture of propane (49 wt%), CO_2 (49 wt%) and water moisture (2 wt%). This unit operation starts with removal of carbon dioxide from propane. This is achieved through gas-scrubbing, a common technique used in carbon capture processes. The gas is passed through an amine-based solvent which chemically absorbs CO_2, and is held in aqueous phase.[21] The solvent is then heated to release CO_2 as a gas stream in a stripping column. Following CO_2 removal, a desiccant-based dehydration unit is in place to remove any remaining moisture in the gas. The dried propane stream is essentially pure, and could be liquefied and stored in gas canisters (150 psi) for transport. Overall, the operating cost of this unit has three portions: desiccant cost, CO_2 capture cost and propane liquefaction cost. The economic assumptions are listed in **Table S19**.

Table S19. TEA assumptions for propane purification

Parameter	**Value**
Carbon capture power cost (kWh/tonne CO_2). Potassium carbonate-based solvent[21]	1167
Compressor specific power (kW/(m^3/h)), 335 psia delivery, propane liquefier	0.5
Desiccant price ($/kg), (desiccant/water ratio = 1/3)	2.6

TEA methodology

Cost estimation

Table S20. Heuristics and empirical correlations for cost estimation.[22, 23]

Heuristics for estimation of working capital WC	
Parameter	**Value**
Working capital	10% ISBL
Heuristics for estimation of fixed capital cost FC	
Parameter	**Value**
Inside battery limit cost (£) for the base case (Case 1)	275,000
FC (£)	500,000
Heuristics for estimation of fixed cost of production FCOP	
Parameter	**Value**
Shift posts	2.69
Operator per shift	4.5
Salary (£ per capita/yr)	25000
Supervision	25% Labour cost
Direct salary overhead	40% (Supervision + labour)
Maintenance	5% ISBL
Property tax	2% ISBL
Rent	2% (ISBL + OSBL)
General plant overhead	65% (Labour + Supervision + Direct salary overhead)
Environmental charge	1% ISBL+OSBL
Exchange rate (GBP to USD)	1.30

Variable costs of production and revenue

The variable costs of production (VCOP) sum up the spending on raw materials, consumables, utilities and other costs that are proportionate with the plant outputs. Revenue is the income generated by selling fermentation products. Key unit prices used for calculating VCOP and revenue have already been summarised in **Table S13**.

Fixed costs of production and working capital

Fixed costs of productions (FCOP), including rent, insurance charge and maintenance, were estimated from capital investment, in addition to labour cost (with £25,000 per shift per year) and related overhead charges. Working capital (WC) covering the plant start-up cost, inventory and accounts receivable/payable were estimated from ISBL.

Economic analysis method

The base case analysis was conducted for a plant designed for 15-years operation. The plant is depreciated using the straight-line method over a 7-year period (i.e. half of the project life). We used the discounted cash flow (DCF) method to evaluate the plant's feasibility. DCF analysis finds the minimum propane selling prices (MPSP) at which propane must be sold in order to generate a net present value (NPV) of zero for a specified hurdle rate by the end of the project (Eq. (5)).

$$\text{NPV} = \sum_{N=1}^{N=t} [CF_N/(1+i)^N] \quad (5)$$

Where i is the hurdle rate and N is the project life in years. CF_N is the cash flow in the Nth year. Major financial assumptions used in TEA are summarised in **Table S21**.

Table S21. Financial assumptions for TEA

Financial assumptions	
Parameter	**Value**
Project length (year)	15
Plant depreciation schedule	Proportional
Depreciation period (year)	Half of project length
Debt ratio	0.4
Equity ratio	0.6
Cost of debt	0.08
Cost of equity	0.11
Hurdle rate	9.80%
Inflation	2%
Construction time (year)	2
% of FC spent in year 1	30
% of FC spent in year 2	70
Startup time (year)	1
% of FCOP during startup	100
% of VCOP during startup	50
% of VCOP during startup	50
Plant salvage value	0
Corporate tax	19%
Operating time (h)	8000
Downtime percentage (%)	20

Results

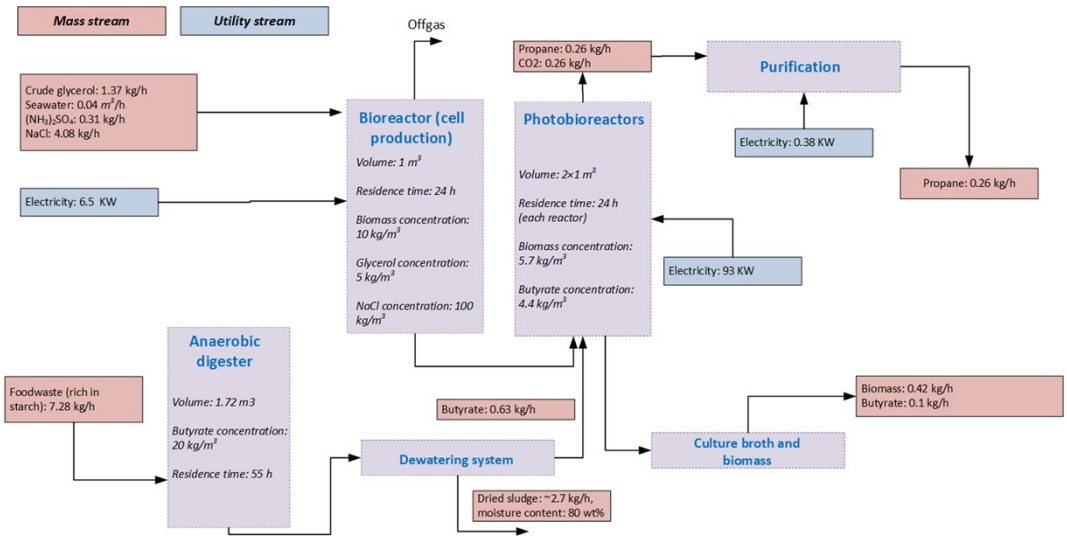

Figure S10. A block flow diagram showing the material inputs/outputs, energy inputs and key system parameters for the base case.

Base case

TEA was performed for the base case scenario with the design basis and assumption presented in Section 2 and 3, respectively. Process balance along with key system parameters are shown in the following block flow diagram (**Fig. S10**)

MPSP, FC, WC, production costs as well as the cost breakdown are calculated and shown in **Table S22**. The basic, non-optimised technology is found to be economically unviable because of high projected MPSP and production cost, which have far exceeded the acceptable range of market selling price ($0.25-1.5/kg, >90% purity). FCOP accounts for nearly 90% of the overall production cost, while the remaining 10% of the cost due to VCOP comes mainly from the electricity consumption during process operation

Table S22. Summary of the TEA of propane production (base case)

VCOP - Raw materials (K$/yr)	13.32
VCOP - Consumables ($/yr)	1.75
VCOP - Electricity ($/yr)	132.04
FC (K$)	650
WC (K$)	65
FCOP (K$/yr)	1,173
Propane production (kg/yr)	2,106
Variable production cost ($/kg propane)	69.86
Fixed production cost ($/kg propane)	556.94
MPSP ($/kg propane)	714.65

Further case studies

In light of the significant gap between the early-stage research and commercial realisation, additional case studies have been created based on the base case by including various options for improvement, as listed in **Table S23**. These case studies serve to highlight the bottlenecks and hotspots, which may have significant impact on the operation of the process, so that future research and process design can be directed in the most effective direction. Addressing the corresponding technical, financial or engineering challenges would be the key to render this process economically viable. The TEA results are summarised in **Table S24**.

Table S23. Descriptions of further case studies developed from the base case.

Case No.	Description
1	Base case. Sterile medium made up with clean process water is used in the continuous fermentation system, while propane is produced as the sole fermentation product.
2	[Case 1] + Introduction of a constitutively expressed chromosome integrated strain to eliminate the use of antibiotics and IPTG induction to ensure stable production of propane.
3	[Case 2] + seawater instead of tap water and non-sterile fermentation conditions
4	[Case 3] + multigene pathway from glycerol to butyrate in *Halomonas* to eliminating the need to source butyrate from AD processes.
5	[Case 4] + co-production of other value-adding commodities (i.e. aquafeed and ectoine).
6	[Case 5] + Electricity sourced from onshore wind turbines instead of via fossil fuels.
7	[Case 6] + improvement of the specific propane productivity of cells by 10-fold (0.0288 → 0.288 g/gDCW•h) – similar to *Halomonas* cell growth / secondary metabolite production optimisation trials described previously.
8	[Case 7] + improvement of cell density in the reactor by 2-fold (10→20 g/L)
9	[Case 8] + Scaling up the production system by 10-fold, assuming the rule of six-tenth for FC

	estimation
10	[Case 9] + construction of the plant in Asian developing countries (e.g. India) with reduced capital (60%), utility/material (40%) and labour cost (20%).
11	[Case 10] + Further reduction of the illumination cost in PBRs by 75% through utilisation of solar energy. Installation of solar concentrators is required (https://www.nrel.gov/docs/fy16osti/65228.pdf).

Table S24. Summary of the TEA of propane production (all cases). The minimum value of MPSP has been set to $0.25/kg, which is equal to the current propane market price.

Case	MPSP ($/kg)	Propane Revenue (K$/yr)	Aquafeed & Ectoine Revenue (K$/yr)	Propane production (kg/yr)	Variable production cost ($/kg)	Fixed production cost ($/kg)
1	714.65	1,505	0	2	69.86	556.94
2	711.25	1,498	0	2	66.52	556.94
3	710.55	1,496	0	2	65.75	556.94
4	536.65	1,495	0	3	49.37	420.87
5	481.75	1,342	155	3	49.98	420.87
6	456.75	1,273	155	3	24.96	420.87
7	64.45	1,276	155	20	3.63	59.22
8	31.55	1,128	309	36	2.14	32.79
9	0.25	89	3,090	358	2.14	3.60
10	0.25	89	3,090	358	2.14	0.89
11	0.25	89	3,090	358	0.92	0.96

Case	VCOP Raw materials (K$/yr)	VCOP Consumables (K$/yr)	VCOP Electricity (K$/yr)	FC (K$)	WC (K$)	FCOP (K$/yr)
1	13.32	1.75	132.04	650.00	35.71	1,172.80
2	6.29	1.75	132.04	650.00	35.71	1,172.80
3	5.70	0.71	132.04	650.00	35.71	1,172.80
4	3.95	0.43	133.20	650.00	35.71	1,172.80
5	3.95	1.12	134.20	650.00	35.71	1,172.80
6	3.95	1.12	64.49	650.00	35.71	1,172.80
7	4.09	1.45	66.37	650.00	35.71	1,172.80
8	5.58	1.87	69.07	650.00	35.71	1,172.80
9	55.84	18.66	690.74	2,587.70	142.18	1,288.84
10	55.84	18.66	690.74	1,552.62	85.31	319.76
11	55.84	18.66	255.99	1,971	108	345

Table S24 summarises the TEA results for all the 11 case studies, including MPSP, product revenue, FC, WC, FCOP and breakdown of the VCOP. Overall, FCOP remains the major contributor to operating expenses (OPEX) for most of the cases. A step-change in fixed production costs appears first in Case 4, which sees a boost in propane production rate due to the replacement of food waste-derived butyrate with glycerol-derived one. More significant step changes occur in Case 7 and Case 9 where propane production rate is further enhanced by process scale-up and strain engineering. Similar to FCOP, notable reduction in VCOP occurs in Case 4 and 7 due to improved propane production rate. Given that electricity is the majority of VCOP, selection of cheaper sources of electricity (Case 6) and reduction of consumption by utilizing solar power (Case 11) would also

significantly lower the VCOP. From an MPSP viewpoint, effective improvement of the process's economic performance is observed in Case 5 (besides Case 4, 7, 8 and 9), suggesting the generation of secondary revenue under an integrated biorefinery framework is necessary to increase the cost-effectiveness of the process

Carbon footprint

Table S25. Carbon footprints of propane production (all cases)

Case	Electricity ($kgCO_2$/yr)	NaCl ($kgCO_2$/yr)	Process water ($kgCO_2$/yr)	Nitrogen source (ammonium sulphate) ($kgCO_2$/yr)	$kgCO_2$/kg Propane
1	154,383	6,535	10	2,969	77.83
2	154,383	6,535	10	2,969	77.83
3	154,383	6,535	10	2,969	77.83
4	155,738	6,535	10	2,969	59.30
5	156,913	6,535	10	2,969	59.72
6	16,286	6,535	10	2,969	9.26
7	16,760	6,535	10	2,969	1.33
8	17,443	6,428	10	5,937	0.83
9	174,429	64,285	100	59,371	0.83
10	174,429	64,285	100	59,371	0.83
11	64,643	64,285	100	59,371	0.53

For the different TEA case studies, we also computed cradle-to-gate carbon footprints, which primarily include emissions due to the utilization of salts (i.e. NaCl and $(NH_4)_2SO_4$ as used in the culture medium), process water and electricity during operation, in hope that this can be used as a starting point for any wider work to reduce the process's emission (**Table S25**). So far, the biggest source of CO_2 emission of the process is the utilization of fossil-fuel derived electricity, given the energy-intensive nature of the artificially illuminated PBR system. Hence, moving to cleaner solar (Case 11) or wind power (Case 6) can be an effective way to reduce not only the operating costs, but the carbon emission as well.

Table S26. List of parameters and their respective bounds for sensitivity analysis

	Unit	Base value	Lower bound	Upper bound	% Variable change
Crude glycerol price	$/kg	0.113	0.0791	0.1469	-30 to 30
Specific propane productivity	kg/kgCell-h	0.288	0.2016	0.3744	-30 to 30
Process scale (using the bioreactor working volume as the basis)	(m3)	10	5	15	-30 to 30
Plant life	(year)	15	10	20	-33 to 33
Hurdle rate	(%)	9.8	7	15	-30 to 50
Total Capital investment	(%)	100	80	120	-20 to 20

Sensitivity study

To better understand the uncertainties of the process economics, one-at-a-time sensitivity analysis was conducted based on Case 11 for variables regarding finances and some of the major improvements suggested by the TEA (**Table S26**).

Figure S11 compares the sensitivity of the various factors on the total annualized cost (TAC) per unit mass of propane produced. The TAC is defined as:

$$TAC = VCOP + FCOP + ACC \quad (5)$$

Where ACC stands for annualized capital charge, as given by Eq. (6):

$$ACC = FC\frac{r}{1-(1+r)^{-n}} \quad (6)$$

Where r stands for hurdle rate, and n is the number of years the project can last for.

The variation of TAC per unit mass of propane due to variable uncertainties is shown in **Figure S11**, where a steeper line indicates a stronger impact.

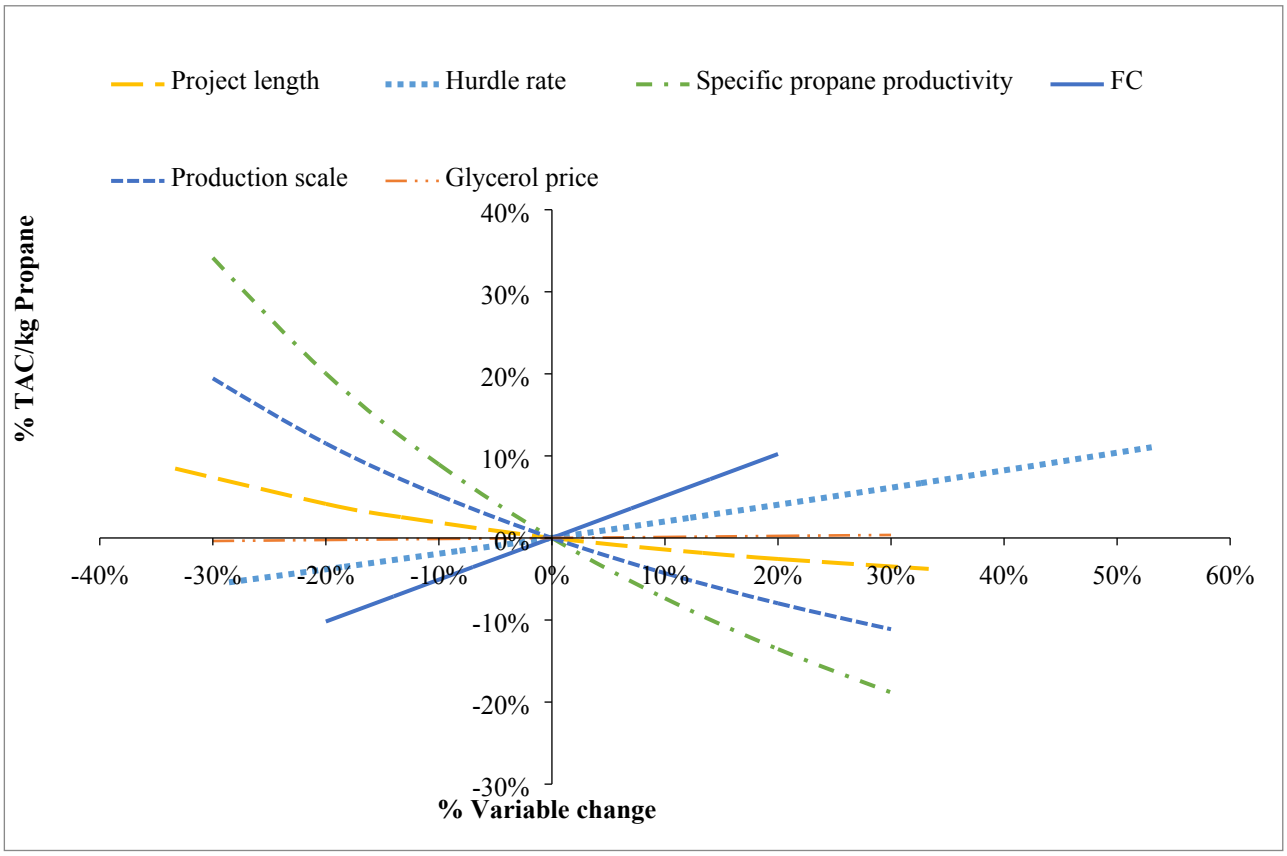

Figure S11. Spider chart for sensitivity analysis for process variables

Amongst the variables tested, specific propane productivity has the greatest negative impact on TAC/kg propane, followed by production scale and project length. Increasing these variables, especially propane productivity, could prove vital for strengthening the process's economic viability. On the other hand, high fixed capital cost and hurdle rate are not favoured as they can easily render the process less viable. In addition, the curve about the price of carbon source (i.e. crude glycerol) is nearly flat, indicating that seeking alternative cheaper feedstock is of little economic significance at this stage.

S2. Statistical analysis of CvFAP variant cell lysate data

Table S8. Analysis by single factor ANOVA indicates that despite high variance in the raw data there is a significant difference between variants with a p-value of 2.22×10^{-1}. Analysis between WT and key variants G462V and G462I by single factor ANOVA indicates there is significant difference between variants (p=0.00143). The high variance in the raw data is likely caused by pH change due to butyric acid addition, differences in the degree of flavination between biological replicates, and in the case of the G462V variant, the presence of an outlier in the biological triplicate data. By two factor ANOVA of the raw data**,** comparing the variation between the CvFAP variants and the 3 biological repeats indicates there is a statistically significant amount of variation between variants ($p=1.63 \times 10^{-25}$) but not between biological repeats (p=0.596). However, comparing the raw data from the pH-controlled assays (**Table S10**) using an identical 2-way ANOVA indicates there is still significant variation between the three key CvFAP variants ($p=7.50 \times 10^{-5}$) and crucially even less chance of statistically significant variation between biological repeats (p=0.846). From these two-way ANOVA tests, we concluded that pH was a source of some variation due to the increase in p value between biological repeats ($\Delta p = 0.846-0.596 = 0.25$).

Given the unequal variance due to the uncontrolled changes in pH in **Table S8**, a t-test assuming equal variances would not be appropriate in this case and an unpaired Welch's t-test[24] would be more appropriate. By Welch's t-test using one tail there is no significant increase by any of the variants compared to wild-type. There is a high degree of variation associated with the errors (standard deviation) in **Table S8**. For example, for wild-type the standard deviation is 35.8% of the mean, for G462V this value is 87.7% whereas for G462I this value is 11.0%. These three coefficients of variation (https://archive.org/details/cambridgediction00ever_0) suggest pH changes likely had a greater effect on the G462V and WT data that the G462I data.

Table S10. Analysis by single factor ANOVA indicates that there is a significant difference between WT and key variants with a p-value of 8.33×10^{-7}. Errors represent one standard deviation of the data using three biological and technical replicates. Analysis by paired two tailed t-test for means indicates that there is significant difference between the propane productivity of the CvFAP variants in this assay with pH control. The t-test for CvFAP WT vs $CvFAP_{G462I}$ gave P=0.00069 to 2 S.F., while for $CvFAP_{WT}$ vs $CvFAP_{G462V}$ gave P=0.018. The final t-test between $CvFAP_{G462I}$ and $CvFAP_{G462V}$ gave P=0.0048. These three P values are less than 0.05, therefore these differences are statistically significant with 95% confidence. On such a data set with 13 independent groups the use of ANOVA is often recommended and found to be more accurate over multiple t-tests.[25, 26] This may explain why the ANOVA indicated significant difference but the Welch's t-tests do not.

To test the validity of this screening data, two CvFAP enzymes (wild-type and G462I) were purified and the increased activity of the G462I variant over wild-type was confirmed (**Fig. S3**).

References

1. I. S. Yunus and P. R. Jones, *Metab Eng*, 2018, **44**, 81-88.
2. I. S. Yunus, J. Wichmann, W. R., K. J. Lauersen, K. O. and P. R. Jones, *Metab Eng*, 2018, **49**, 201-211.
3. D. Sorigué, B. Légeret, S. Cuiné, S. Blangy, S. Moulin, E. Billon, P. Richaud, S. Brugière, Y. Couté, D. Nurizzo, P. Müller, K. Brettel, D. Pignol, P. Arnoux, Y. Li-Beisson, G. Peltier and F. Beisson, *Science*, 2017, **357**, 903-907.
4. R. Anggit, M. T. Ho and D. E. Wiley, *Ind Eng Chem Res*, 2013, **52**, 16887-16901.
5. G. L. Rorrer, in *Springer Handbook of Marine Biotechnology*, ed. S.-K. Kim, Springer, 2015, pp. 257-294.
6. C. Selim, G. Yilan, B. S. Akbulut, A. Poli and D. Kazan, *J Biosci Bioeng*, 2012, **114**, 45-52.
7. E. A. Tampio, L. Blasco, M. M. Vainio, M. M. Kahala and S. E. Rasi, *GCB Bioenergy*, 2019, **11**, 72-84.
8. S. Ceylan, *J Biosci Bioeng*, 2012, **114**, 45-52.
9. FAO, Food loss and food waste, http://www.fao.org/food-loss-and-food-waste/en/ (accessed 4 September 2019).
10. Wrap, 2016.
11. M. Atasoy, I. Owusu-Agyeman, E. Plaza and Z. Cetecioglu, *Bioresour Technol*, 2018, **268**.
12. H. Ma, H. Liu, L. Zhang, M. Yang, B. Fu and H. Liu, *Biotechnol Biofuels*, 2017, **10**, 1-15.
13. N. Liu, Q. Wang, J. Jiang and H. Zhang, *Renewable Energy*, 2017, **113**, 1523–1528.
14. P.-M. Olivard, MSc, Polytechnic University of Catalonia, 2017.
15. M. Tlusty, A. Rhyne, J. T. Szczebak, B. Bourque, J. L. Bowen, G. Burr, C. J. Marx and L. Feinberg, *PeerJ*, 2017.
16. C. Wang, J. Chuprom, Y. Wang and L. Fu, *J Appl Microbiol*, 2019, **2019**, 1-13.
17. A. Bownik and Z. Stępniewska, *Arh Hig Rada Toksikol*, 2016, **67**, 260–265.
18. S. Karimi, N. M. Soofiani, A. Mahboubi and M. J. Taherzadeh, *Sustainability*, 2018, **10**, 3296.
19. H. Kunte, G. Lentzen and E. Galinski, *Curr Biotechnol*, 2014, **3**, 10–25.
20. J. H. Litchfield, *Adv Appl Microbiol*, 1977, **22**, 267–305.
21. A. Raksajati, M. T. Ho and D. E. Wiley, *Ind Eng Chem Res*, 2013, **52**, 16887–16901.
22. R. Sinnott and G. Towler, *Chemical Engineering Design*, Butterworth-Heinemann, 5 edn., 2009.
23. K. T. Group, General Process Plant (Engineering Design Guideline), http://kolmetz.com/pdf/EDG/ENGINEERING_DESIGN_GUILDLINE_General_Plant_Cost_Estimating_Rev01web.pdf., (accessed 13 March, 2020).
24. B. L. Welch, *Biometrika*, 1947, **34**, 28-35.
25. J. Rojewski, I. H. Lee and S. Gemici, *Career and Technical Education Research*, 2012, **3**, 263-275.
26. S. M. Brady, M. Burow, W. Busch, Ö. Carlborg, K. J. Denby, J. Glazebrook, E. S. Hamilton, S. L. Harmer, E. S. Haswell, J. N. Maloof, N. M. Springer and D. J. Kliebenstein, *The Plant Cell*, 2015, **27**, 2088-2094.